NEW HORIZONS FOR UNCOOLED IR SENSORS

Charles M. Hanson
Raytheon Company, Dallas, TX

ABSTRACT

The performance requirements for space-based IR imaging sensors are generally so severe that uncooled detector technologies have historically been ignored – and rightly so. The reasons for this have often been inaccurately represented on the basis of theoretical analysis with unnecessary assumptions. This paper shows that the performance of uncooled or minimally-cooled IR detectors can approach or even exceed that of cooled photon detectors. It also describes the practical barriers to achieving such performance. A detailed analysis of signal and noise shows that the background-limited performance of a well-designed thermal detector is not much different from that of a photon detector. The analysis also shows that these distinct detector types are optimally suited for different types of applications. The barriers to achieving background-limited sensitivity are quite different for thermal detectors. In this paper we quantify the barriers, and discuss their implications.

INTRODUCTION

Uncooled IR imaging is at last, after some 25 years of development, commonplace. Many companies working with several different technologies are producing a diverse variety of products in quantity. Some products are lower-cost versions of products that have been around for a long time, while other products were difficult to imagine prior to the advent of uncooled IR focal plane arrays (FPAs). The initial measure of viability of these devices was a sensitivity comparable to the poorest of cooled IR sensors. We have seen various technologies mature to the point that FPAs with 320×240 pixels and with pixel sizes on the order of 50 μm perform significantly better than that standard. Larger arrays with smaller pixels are further blurring the boundaries between uncooled and cooled technologies. The words "radiation-limited performance" are now being commonly spoken in reference to development activities for uncooled IR FPAs. What is meant by that is usually the oft-quoted 1.8×10^{10} cm·Hz^{½}/W "ultimate" D^* limit for thermal detectors. Although barriers to achieving that level of performance certainly remain, it by no means represents the ultimate limit for these detectors. The assumptions in the analysis that leads to this magical D^* are non-essential, and are in fact not true of modern micro-machined devices. This, of course, has serious implications for the future of space-based IR imaging sensors.

REVIEW OF FUNDAMENTALS

What we commonly call "uncooled" detectors are better characterized as "thermal" detectors, as opposed to "photon" detectors. A thermal detector is characterized by the fact that its response is proportional to the *amount of energy* in the absorbed photon stream. The response of a photon detector is proportional to the *number* of absorbed photons. In a photon detector, a photon is absorbed directly by the IR-sensitive material, and the charge carriers generated by that absorption are sensed either directly or by a concomitant change in some property of the material. A thermal detector, by contrast, comprises three distinct parts: An IR absorber, a thermal isolation means, and a temperature sensor or transducer, as illustrated in Figure 1. The purpose of the IR absorber is to convert IR electromagnetic energy into heat energy. The thermal isolation, modulated by the thermal mass (heat capacity), converts the heat energy to a temperature change. The transducer converts the temperature change to a change in a measurable (usually electrical) parameter. The three parts of a thermal detector are functionally independent, although the device may be designed in such a manner that they are interdependent.

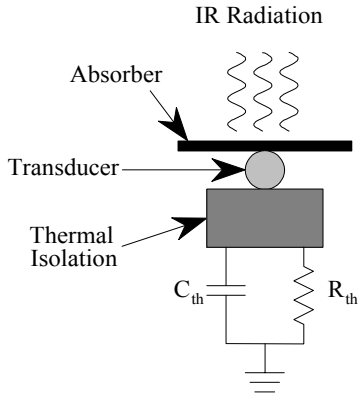

Figure 1 – Schematic view of the constituent parts of a thermal detector.

The voltage responsivity of this generic detector is

Report Documentation Page

Report Date	Report Type	Dates Covered (from... to)
29JUL2002	N/A	-

Title and Subtitle New Horizons for Uncooled IR Sensors	**Contract Number**
	Grant Number
	Program Element Number
Author(s)	**Project Number**
	Task Number
	Work Unit Number
Performing Organization Name(s) and Address(es) Raytheon Company Dallas, TX	**Performing Organization Report Number**
Sponsoring/Monitoring Agency Name(s) and Address(es)	**Sponsor/Monitor's Acronym(s)**
	Sponsor/Monitor's Report Number(s)

Distribution/Availability Statement
Approved for public release, distribution unlimited

Supplementary Notes
See Also ADM201460. Papers from Unclassified Proceedings from the 11th Annual AIAA/MDA Technology Conference held 29 July - 2 August 2002 in Monterey, CA.

Abstract

Subject Terms

Report Classification unclassified	**Classification of this page** unclassified
Classification of Abstract unclassified	**Limitation of Abstract** UU

Number of Pages
9

$$R = \frac{\alpha_{abs}}{G_{th}}\left(\frac{dV}{dT}\right)\frac{1}{\sqrt{1+\omega^2\tau_{th}^2}} \ , \qquad (1)$$

where α_{abs} is the absorptivity (absorption efficiency), G_{th} is the thermal conductance ($G_{th} = 1/R_{th}$), (dV/dT) is the (voltage) response of the detector material per unit detector temperature change, ω is the angular frequency of modulation of the signal, and τ_{th} is the thermal time constant.

Noise comes from a variety of sources. If the level of the noise at the output of the focal plane is not amplified to a sufficient level, the sensor may be limited by system noise. This can usually be overcome by conscientious design of the system and readout integrated circuit (ROIC). The ROIC itself may contribute sufficient noise to dominate performance. This is especially true for smaller pixels, because smaller IC devices tend to have relatively higher noise. Additionally, several noise sources originate in the detector itself. These include Johnson (or thermal) noise, current noise (typically 1/f), and temperature-fluctuation noise. The last of these is peculiar to thermal detectors, although it is not unrelated to shot-noise phenomena in photon detectors.

Temperature-fluctuation noise is the random variation of the detector temperature resulting from fluctuation in the exchange of heat with the environment. The spectral density of this variation is given by

$$\overline{\delta T(\omega)}^2 = \frac{4k_B T^2}{G_{th}}\frac{1}{1+\omega^2\tau_{th}^2} \ . \qquad (2)$$

Note that this noise is band limited by the thermal time constant in the same manner as the responsivity. When integrated, the net temperature fluctuation is

$$\delta T = \sqrt{\frac{k_B T^2}{C_{th}}} \ , \qquad (3)$$

where C_{th} is the heat capacity ($\tau_{th} = R_{th}\, C_{th} = C_{th} / G_{th}$). The resulting output noise voltage is then

$$v = \left(\frac{dV}{dT}\right)\sqrt{\frac{k_B T^2}{C_{th}}} \ , \qquad (4)$$

and the noise-equivalent power (NEP) at low frequency is

$$NEP = \frac{G_{th}}{\alpha_{abs}}\sqrt{\frac{k_B T_d^2}{C_{th}}} = \frac{1}{\alpha_{abs}}\sqrt{\frac{k_B G_{th} T_d^2}{\tau_{th}}} \ . \qquad (5)$$

Figure 2 shows the dependence of NEP on G_{th}.

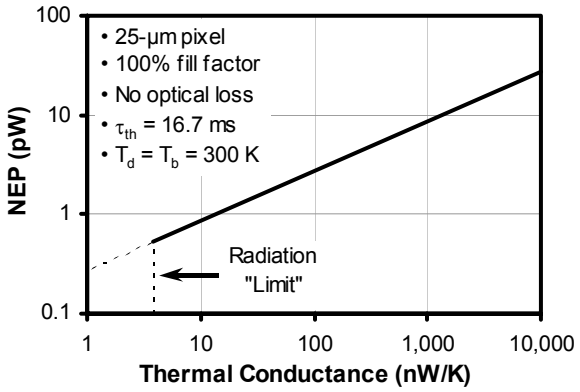

Figure 2 - Dependence of limiting NETD on thermal isolation.

The rate of heat exchange between the detector and its environment is

$$W = G_{cond}(T_d - T_b) + \sigma_B(T_d^4 - T_b^4)A_d \ , \qquad (6)$$

where G_{cond} is the mechanical thermal conductance, σ_B is the Stefan-Boltzmann constant, T_b is the background/ambient temperature, and A_d is the detector active area.

The second term in Eq. (6) is the radiation term. If radiation dominates, then the conductance is said to be radiation-limited, and the effective thermal conductance is

$$G_{rad} = \frac{dW_{rad}}{dT_d} = 4\sigma_B T_d^3 A_d \ . \qquad (7)$$

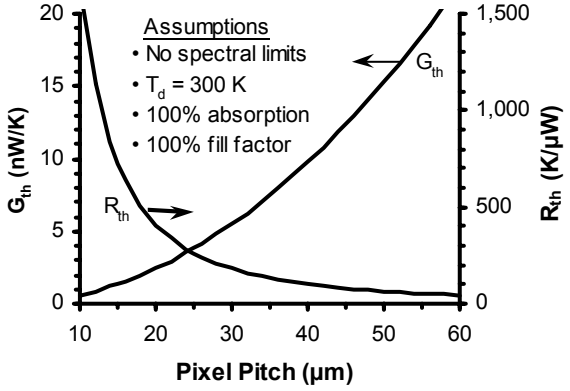

Figure 3 - Dependence of broadband radiation-limited thermal conduction/resistance on pixel size.

Figure 3 shows how pixel size affects the limiting thermal isolation. Both the radiation-limited thermal conductance and the thermal mass (heat capacity) scale linearly with detector area, so the thermal time constant is independent of area. This is not the case if

mechanical conduction dominates, because mechanical conduction does not generally scale with area. In fact, this is a primary difficulty in achieving radiation-limited thermal conductance in small pixels. If we reduce pixel pitch by a factor of two, maintaining constant fill factor, then we must also reduce the thermal conductance by a factor of *four* to maintain a given thermal time constant. For a typical microbridge structure, scaling by a factor of two affects the support arm length and width by the same factor, so the thermal isolation is not affected. Since the arm width is often the critical dimension for photolithography, it becomes significantly more difficult even to maintain the nominal thermal isolation. Further improvements beyond the basic shrinking of the pixel are necessary to maintain radiation-limited thermal isolation.

It is probably worthwhile to point out some analogies with photon detectors. The radiation limit is, of course, analogous to the background limit for photon detectors. In the case of photon detectors, background photons generate charge carriers in the detector material, creating a photocurrent. At the same time, thermal processes within the detector material also generate carriers, creating dark current. Each of these currents has an associated shot noise resulting from random fluctuations in the generation rate (and, in some cases, recombination) of these carriers. If this shot noise dominates, and if the background photocurrent is greater than the dark current, then the device is said to be background limited. In the case of thermal detectors, we deal with heat flow and temperature rather than electric current and charge carriers. A thermal detector exchanges radiation with its environment (background), resulting in a temperature change. Also, heat may flow to and from the detector by thermal conduction and/or convection. Each of these heat exchange mechanisms has an associated fluctuation because of the random nature of the processes involved, and the result is known as temperature fluctuation noise. If this noise dominates, and if the radiant heat exchange is greater than that from conduction and convection, then the device is said to be radiation limited.

THERMAL VS. PHOTON DETECTORS

Some have suggested the possibility of the operation of photon detectors near normal ambient temperature as a technology potentially competitive with "uncooled" thermal detectors. There are certain advantages of such a device, if it is indeed feasible. A thermal detector requires a nominal vacuum package for the purpose of eliminating the contribution of air conduction to the total thermal conductance. An IR photon detector normally requires a vacuum package for other reasons. Since the detector must be cooled (based on current technologies), the vacuum package is necessary to reduce thermal loading on the cooling device and to eliminate the possibility of condensation on the detector itself. An IR photon detector capable of efficient operation without cooling would eliminate both of these issues and therefore eliminate the need for a vacuum package. Furthermore, such a photon detector would not require thermal isolation, and it would likely be capable of operation at much higher frequencies than thermal detectors. Of course, no one really knows how to make an IR photon detector capable of background-limited operation without cooling.

A thermal detector has its own advantages, the principle one being the relative crudeness of the detector material requirements. Thermal detectors generally depend upon macroscopic material properties, whereas photon detectors generally depend upon microscopic properties. This has important implications regarding the cost to produce. Of course, no one really knows yet how to make a background-limited thermal detector.

The intent of this section is to evaluate the limiting performance of thermal detectors as compared to photon detectors. For photon detectors we are concerned with the number of photons absorbed from a blackbody source. The number of background photons absorbed is given by

$$n = 2\pi c A \tau_{\text{int}} \int_0^\infty \frac{\alpha(\lambda)}{\lambda^4} \left(e^{hc/\lambda k_B T_b} - 1 \right)^{-1} d\lambda \ , \qquad (8)$$

where τ_{int} is the integration time, and $\alpha(\lambda)$ is the spectral absorptivity.

For a thermal detector we are concerned with the rate at which heat is absorbed from a blackbody source. That rate is

$$W = 2\pi hc^2 A \left\{ \int_0^\infty \frac{\alpha(\lambda)}{\lambda^5} \left(e^{hc/\lambda k_B T_b} - 1 \right)^{-1} d\lambda - \right. \\ \left. - \int_0^\infty \frac{\alpha(\lambda)}{\lambda^5} \left(e^{hc/\lambda k_B T_d} - 1 \right)^{-1} d\lambda \right\} \qquad (9)$$

where the second term accounts for radiation emitted by the detector into its environment. Now the signals for the two detector types are proportional, respectively, to the derivatives of Eqs. (8) and (9) with respect to background temperature,

$$\partial n / \partial T_b = \\ \frac{\pi}{2} \frac{hc^2}{k_B T_b^2} A \tau_{\text{int}} \int_0^\infty \frac{\alpha(\lambda)}{\lambda^5} \operatorname{csch}^2 \left(hc / 2\lambda k_B T_b \right) d\lambda \qquad (10)$$

and

$$\partial W/\partial T_b = \frac{\pi}{2}\frac{h^2c^3}{k_B T_b^2} A \int_0^\infty \frac{\alpha(\lambda)}{\lambda^6} \operatorname{csch}^2\left(hc/2\lambda k_B T_b\right) d\lambda \quad (11)$$

where we have used hyperbolic function notation to simplify the appearance.

Equations representing the noise due to the random exchange of photons with the environment can be derived from consideration of quantum statistical mechanics of the radiation field. There is, however, a key difference between photon detectors and thermal detectors. In thermal detectors, the random emission of photons from the detector affects its temperature fluctuation in the same manner as the random absorption of photons emitted by the environment. For a photon detector, at least for a photodiode, only the random absorption from the background contributes. The equations are

$$\overline{\Delta n}^2 = \frac{\pi}{2} cA\tau_{\text{int}} \int_0^\infty \frac{\alpha(\lambda)}{\lambda^4} \operatorname{csch}^2\left(hc/2\lambda k_B T_b\right) d\lambda \quad (12)$$

and

$$\overline{\Delta W}^2 = \pi h^2 c^3 A \Delta f \left\{ \int_0^\infty \frac{\alpha(\lambda)}{\lambda^6} \operatorname{csch}^2\left(hc/2\lambda k_B T_b\right) d\lambda + \int_0^\infty \frac{\alpha(\lambda)}{\lambda^6} \operatorname{csch}^2\left(hc/2\lambda k_B T_d\right) d\lambda \right\} \quad (13)$$

since absorptivity equals emissivity. Here Δf is the noise bandwidth. The noise bandwidth is not explicitly noted in Eq.(12) because it is implicit in the integration time. It should be noted that these two equations assume only one active detector surface. This is valid for a thermal detector that makes use of a resonant absorption structure, but a photon detector will also absorb photons generated by its substrate, and this will increase Eq. (12) by approximately a factor of two when $T_d \approx T_b$, unless the backside is reflective. Clearly, if we reduce the temperature of the thermal detector sufficiently, we can eliminate the contribution of the second integral in Eq. (13). Figure 4 and Figure 5 give an indication of the temperature to which we must reduce the detector to achieve this result. In Figure 4, which plots the integrand of Eq.(13), it is clear that the noise peak decreases with decreasing temperature, and it shifts to longer wavelengths. It is easier to make quantitative evaluations using Figure 5, which is actually a top view of Figure 4 shown with contours. The contours at the top of the figure represent higher noise values than those in the lower parts. The minima of the curves occur at wavelengths for which noise is a maximum for the temperature at which the minimum occurs. This becomes obvious if you draw a horizontal line through one of the minima, and realize that every point below a given contour represents lower noise than the points on the contour. The upper darker line is the curve appropriate to the spectral noise peak at 300 K. In general, the noise maxima occur at

$$\lambda_{\max} = \frac{hc}{5.969\, k_B T} \ . \quad (14)$$

For T = 300 K, λ_{max} = 8.035 μm; at T = 240 K, λ_{max} = 10.043, and the peak value is reduced by about a factor of two. The lower dark contour in Figure 5 is the line for which the noise is exactly half that of the upper dark contour. Its minimum is at about 240 K and 10 μm.

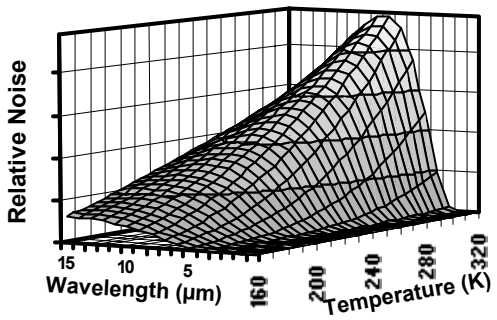

Figure 4 - Contour of spectral noise contributions as a function of temperature and wavelength, for a thermal detector.

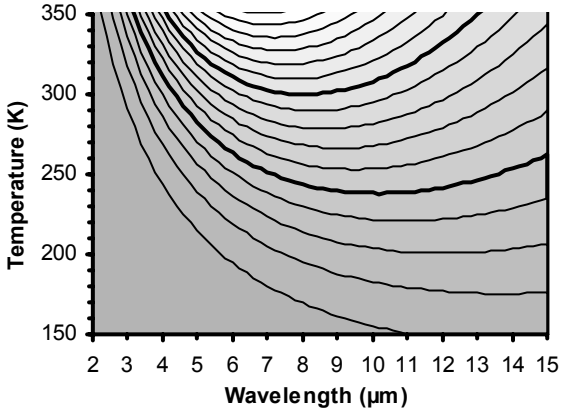

Figure 5 - Lines of constant noise, as a function of wavelength and temperature. Bold lines indicate two contours whose emission contribution to noise differs by a factor of two.

Thus, by reducing the detector temperature to 240 K, we reduce its emission noise by about one-half. Since this adds in quadrature with the absorption noise, the net result is degradation from the ideal background limit by only about 12%. This has important consequences in what follows.

The signal-to-noise ratio for a photon detector is obtained by dividing Eq. (10) by the square-root of Eq. (12); and that for a thermal detector, by dividing Eq. (11) by the square-root of Eq. (13). Doing this wouldn't give us much insight, but if we limit the spectral band to a narrow region, we obtain

$$\frac{1}{\Delta n_\lambda}\frac{\partial n_\lambda}{\partial T} = \sqrt{\frac{\pi}{2} cA\tau_{\text{int}}\alpha(\lambda)\Delta\lambda}\,\frac{hc}{k_B T_b^2}\frac{1}{\lambda^3}\,\text{csch}\left(hc/2\lambda k_B T_b\right) \tag{15}$$

and

$$\frac{1}{\Delta W_\lambda}\frac{\partial W_\lambda}{\partial T} = \sqrt{\pi\, cA\tau_{th}\alpha(\lambda)\Delta\lambda}\,\frac{hc}{k_B T_b^2}\times \times\frac{1}{\lambda^3}\frac{\text{csch}^2\left(hc/2\lambda k_B T_b\right)}{\sqrt{\text{csch}^2\left(hc/2\lambda k_B T_b\right)+\text{csch}^2\left(hc/2\lambda k_B T_d\right)}} \tag{16}$$

In comparing Eqs. (15) and (16), we observe a few differences. They each depend on a time constant, but the time constants are different, and there is an additional factor of two. These differences occur because the photon detector is assumed to be characterized by an integration time τ_{int}, whereas the thermal detector is assumed to be characterized by the roll-off of a single-pole filter whose time constant is τ_{th}. The bandwidth for in integrator is

$$\Delta f_{\text{int}} = \frac{1}{2\tau_{\text{int}}} \ , \tag{17}$$

whereas that for a single-pole filter is

$$\Delta f_{th} = \frac{1}{4\tau_{th}} \ , \tag{18}$$

which accounts for the apparent factor of two, when we consider that we should compare devices of similar bandwidth. For an infrared photon detector τ_{int} is typically very short – measured in tens or perhaps hundreds of microseconds. For a thermal detector it is longer – typically longer than 10 milliseconds. The photon detector therefore has a speed advantage; the thermal detector, a sensitivity advantage, in principle. Of course, a system using a photon detector can integrate multiple high-speed frames off focal plane, but there will usually be a net loss due to cycle time efficiencies. Also, a thermal detector can operate at higher speeds, with a concomitant loss of sensitivity very similar to that observed in photon detectors.

Another notable difference is that if the detector temperature is equal to the background temperature, then the thermal detector signal-to-noise ratio is degraded by $\sqrt{2}$ relative to that of an ideal photon detector. Note also that if the emission noise term in Eq. (16) is negligible, then the two equations are identical. The importance of the earlier analysis is that it is only necessary to cool a thermal detector to 240 K to remove this $\sqrt{2}$ penalty. Of course this is only valid if the radiation limit still applies at the reduced temperature. There is a slight error in comparing Eqs. (15) and (16) for a broad spectral range, because the integral of a ratio is not equal to the ratio of integrals. However, for reasonable spectral bands the error is typically less than a few per cent.

Why then does the conventional wisdom maintain that thermal detectors will always be substantially inferior relative to photon detectors? The answer to this question lies in previous assumptions made regarding Eq. (13). The past pessimistic projections have assumed that $\alpha(\lambda)$ is unity, or at least constant, over the entire spectrum. For constant $\alpha(\lambda)$, Eq. (13) becomes

$$\overline{\Delta W}^2 = 8\alpha\sigma_B k_B\left(T_d^5 + T_b^5\right)A_d\,\Delta f \ . \tag{19}$$

where σ_B is the Stefan-Boltzmann constant, given by

$$\sigma_B = \frac{2\pi^5}{15}\frac{k_B^4}{h^3c^2} \ . \tag{20}$$

Eq. (19) is the usual equation given for radiant noise power in a thermal detector. The NEP in this case is given by

$$NEP = \frac{1}{\alpha}\sqrt{\overline{\Delta W}^2} = \sqrt{\frac{8\sigma_B k_B\left(T_d^5 + T_b^5\right)A_d\,\Delta f}{\alpha}} \tag{21}$$

where the $1/\alpha$ factor is present to convert from absorbed power to incident power. For $\alpha = 1$ and $T_d = T_b = 300$ K, this results in a blackbody D^* of 1.813×10^{10} cm·Hz$^{1/2}$/W. Limiting the spectral band to between 8.0 µm and 13.0 µm reduces the noise and thereby increases D^* by more than 50%.

Thus, we see that the key to improving thermal detector performance to the level of photon detector performance is limiting the spectral band over which it absorbs and emits radiant noise to correspond to that over which it absorbs signal. A photon detector does this automatically by virtue of its band gap. In time past, great pains were taken to give thermal detectors

broad spectral response – indeed, this was one of their primary advantages. Modern thermal detectors, however, are made very small to facilitate high-resolution imaging. This necessitates a high degree of thermal isolation to maintain high sensitivity, and this in turn requires low thermal mass. Broad-band spectral absorbers are not generally compatible with such low-mass structures. Most modern devices use a resonant optical absorber, which is a low-mass means to provide excellent absorption over a spectrum that can be adjusted by simply changing the gap between the device and the substrate. This provides without encumbrance a restriction of the spectral band that can contribute to temperature-fluctuation noise.

BARRIERS

From the earlier discussions it is clear that minimizing net thermal conductance is of paramount importance to improving the performance of thermal detectors. In the following subsections we will discuss some of the limitations to such reductions and the implications on device and package design.

Thermal Conductance

Just as a change of band gap and cold-shielding can improve the performance of photon detectors, so also can a reduction in absorbed background radiation improve thermal detectors. There are several straightforward techniques that will accomplish this, some of which have already been mentioned. First, limiting the spectral response as nearly as possible to the bandwidth of interest for signal can have a substantial effect. For example, For a device whose signal spectral band is from 8.0 µm to 12.0 µm, eliminating all out-of-band radiation reduces the radiant thermal conductance by a factor of 2.6. Second, limiting the field of view of the detector by "cool shielding" can significantly reduce the effective thermal conductance. For an *f*/1.0 optical system, 75% of the radiation that strikes the detector comes from outside the system field of view. For larger *f*/numbers the fraction is even greater. Elimination of radiation from this region could reduce the thermal conductance by a factor of 4 or more, depending on the detector temperature. As implied by the term "cool shield" (as contrasted with "cold shield"), even a modest reduction in the shield temperature can produce important improvement. Third, reducing the detector temperature can eliminate its emissions as a measurable source of noise.

All of these improvements are simple in principle, and mostly in practice. Band limiting occurs naturally in most low-mass absorbers. Although the technology for "cool shielding" is readily available, it could adversely affect cost-sensitive products. Reduction of the detector temperature is easily accomplished by using a two- or three-stage thermoelectric cooler. This, also, will add to the detector cost.

Just as reducing the absorbed background radiation improves the performance of photon detectors only if background current is a significant contribution to total current, so also does reducing the radiant thermal exchange improve the performance of thermal detectors only if radiant thermal exchange is a significant contribution to total thermal exchange. As one limits the spectral band and implements radiation shielding, the radiant contribution to thermal conduction diminishes. At some point, radiant exchange will be dominated by other heat exchange processes, and further reduction in the radiant component will produce little or no benefit. This is analogous to reducing photodetector background radiation to the point that dark current strongly dominates. In that case, further reduction of the background will not substantially improve performance. Therefore, the need to improve the mechanical implementation to minimize thermal conduction becomes ever more important as one reduces the radiant component.

Heat Capacity

The thermal time constant is related to the pixel heat capacity and thermal conductance as follows:

$$\tau_{th} = \frac{C_{th}}{G_{th}} \ . \tag{22}$$

This means that the heat capacity must be reduced concomitantly with the thermal conductance, in order to maintain a useful time constant. The heat capacity is given by

$$C_{th} = \rho c_p A_d z_d \ , \tag{23}$$

where ρ is the average density of the pixel, c_p is the average specific heat, A_d is the detector physical area, and z_d is the average detector thickness.

Using these two equations with Eq. (7), we get

$$\tau_{th} = \frac{\rho c_p z_d}{4\sigma_B T_d^3} \ . \tag{24}$$

The only independent physical parameter in this equation is z_d; so this places a constraint upon the thickness of the detector structure. Figure 6 shows that a time constant of 1/60 sec dictates that the structure thickness be only 340 Å, assuming an average ρc_p of

3.0 J/cm^2. This actually overestimates the allowed thickness, because the thermal isolation structure also contributes half its mass to the heat capacity. Within this thickness the pixel must also contain an IR absorption structure.

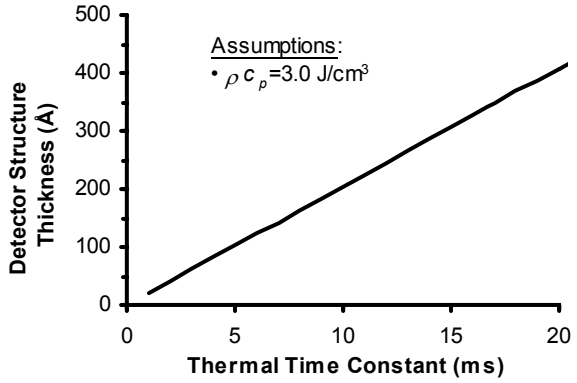

Figure 6 - Relationship between detector structure thickness and thermal time constant for a radiation-limited detector.

Vacuum Package

The detector pixel can exchange heat with its environment by thermal conduction through the gas in its container. This imposes a constraint on the package vacuum level. It is apparent that the conduction path between the pixel and the ROIC will be most important, because the spacing is typically only about 2 µm. However, at low pressures, the mean-free path can be significantly longer than the spacing between the pixel and the window, which is typically about 500 µm. Therefore, under low-pressure conditions the pixel-to-window conduction path will contribute equally with the pixel-to-ROIC path. The effective mean-free path is given by

$$\lambda(L) = \left[\frac{\sqrt{2}\pi P d^2}{k_B T} + \frac{1}{L} \right]^{-1} , \qquad (25)$$

where P is the pressure, d is the molecular diameter of the conducting gas (3.14 Å for N_2), and L is the spacing between the pixel and the surface under consideration.

Adding the *1/L* term is an approximation that assumes the inter-molecular and surface collision rates are additive. The effective thermal conductivity for N_2 is

$$k_g(L) = \frac{7}{4} P \sqrt{\frac{8 k_B N_A}{\pi M T}} \lambda(L) , \qquad (26)$$

where N_A is Avagadro's number, and M is the molar mass (28 gm for N_2).

The net thermal conductance contributed by the gas is

$$G_{gas} = \left[\frac{k_g(L_s)}{L_s} + \frac{k_g(L_w)}{L_w} \right] A_d , \qquad (27)$$

where L_s is the pixel-to-substrate distance, and L_w is the pixel-to-window distance.

Figure 7 below shows the results for 25 µm pixels. The two contributions are roughly equal below about 50 mTorr. Since the gas conductance is proportional to the detector area, the ratio of gas conductance to radiative conductance is independent of pixel size. For N_2, gas conductance is equal to radiative conductance at a pressure of about 8 mTorr. Since, according to Figure 7, the gas thermal conductance is proportional to pressure at low pressure, the package pressure must be below about 2 mTorr to keep the NETD degradation due to gas conduction at about 10%. (Conductances add linearly, and NETD varies as the square-root of total conductance.)

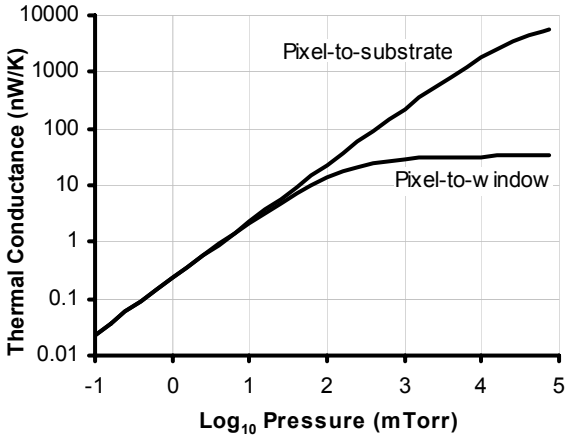

Figure 7 – Contributions of gas thermal conductance as a function of pressure.

Electrical Resistance

The structure that provides thermal isolation must also provide mechanical strength as well as an electrically conductive path for accessing signals generated by the detector. These are not independent features, and we will consider in particular the relationship between electrical conductance and thermal conductance. The support structure generally comprises two elements, an electrically insulating mechanical layer and an

electrically conductive layer. For the purposes of this analysis we will assume that the electrically conductive layer dominates the thermal conductance. This is probably a good approximation for well-designed small structures in which the mechanical demands are not too severe. In the electrically conductive layer the thermal conductance and the electrical resistance are linked by the Wiedemann-Franz relationship,

$$G_{th}R_e = k\rho > \frac{\pi^2}{3}\left(\frac{k_B}{q}\right)^2 T = 7.35\,\frac{\mu\mathrm{W}\cdot\Omega}{\mathrm{K}}\ , \qquad (28)$$

where G_{th} is the thermal conductance, R_e is the electrical resistance, k is the thermal conductivity, and ρ is the electrical resistivity.

The ">" is present instead of the "=" sign because the Wiedemann-Franz law applies strictly only to electron transport. Since phonons can contribute significantly to thermal transport but not directly to electron transport, the Wiedemann-Franz law is a lower limit to the thermal conductivity. The expression "$G_{th}R_e$" reduces to "kρ" because geometrical factors exactly cancel.

We require that the thermal conductance of the support structure be much less than that due to radiative exchange, so

$$G_{th} << 4\sigma_B T^3 A_d \quad \Rightarrow \quad R_e >> \frac{7.35\,\frac{\mu\mathrm{W}\cdot\Omega}{\mathrm{K}}}{4\sigma_B T_d^3 A_d} = 1.92\,\mathrm{k}\Omega$$

If we allow the support structure to contribute 20% to the total thermal conductance, then we have $R_e > 10\ \mathrm{k}\Omega$ for a 10% impact to NETD. The resistance needs to be even higher if the electrically conductive material is a poor conductor or if the thermal conductance contribution of the mechanical structure is non-negligible.

This has serious consequences for low-impedance detectors such as thermocouples or low-resistance bolometers. For a bolometer of resistance R_d, a series resistance of R_s degrades the effective temperature coefficient of resistance (TCR) by

$$\alpha_{eff} = \frac{1}{R_d + R_s}\frac{d}{dT}\left(R_d + R_s\right) = \\ = \frac{1}{R_d + R_s}\frac{dR_d}{dT} = \frac{R_d}{R_d + R_s}\alpha \qquad (29)$$

Therefore a 10 kΩ bolometer with a 10 kΩ series resistance would have an effective TCR of half its nominal value. For pyroelectric detectors or bolometers with resistance greater than about 100 kΩ, the impact is negligible.

Spatial Noise

Detector pixel signal-to-noise ratio is not the only parameter important to target acquisition and surveillance. As sensitivity improves, other issues become more important. The issue of paramount importance in most modern uncooled IR imaging sensors is spatial noise. Spatial noise has three fundamentally different causes: Offset non-uniformity, response non-uniformity, and low-frequency noise. Offset variation among the detector pixels is the greatest contributor to raw non-uniformity. In bolometers this results primarily from pixel-to-pixel resistance variation. This non-uniformity is readily corrected, but it greatly increases the electronic complexity of the device. Subtle changes such as slight drift of the focal plane temperature or bias voltage give rise to unacceptable non-uniformity even after the baseline correction, so the correction coefficients must be updated periodically, which requires obscuration of the image for a short time every few minutes. Alternatively, offset non-uniformity can be obviated by use of a chopper with a detector having AC-coupled pixels. A chopper can also be effective with a DC-coupled detector, but only with substantial performance penalty.

The problems arising from gain non-uniformity are not usually as severe a problem as those from offset non-uniformity, but it must also be corrected. Its greatest impact to performance arises when the average temperature of a region of the scene is substantially different from that for which the sensor was initially calibrated. If such a scene were uniform, then the non-uniform response of the array would make the image appear non-uniform or cluttered. If such a scene were complex, the non-uniformity would add clutter or shading. Gain uniformity is usually very easily corrected unless the detector response is significantly non-linear, and the correction coefficients are usually highly stable.

Low-frequency noise is manifest as slowly-changing spatial noise, and this is particularly so for 1/f noise[1]. Signal and noise measurements are generally made by taking data samples over a period of up to one second. Noise components at frequencies substantially lower than one Hertz are not at all evident in such measurements. If the same measurements were taken a minute or an hour later, the noise would appear the same, but the offsets would appear to be different. The low-frequency noise components would have changed *between* measurements, but they do not change *during* the measurements. Because each pixel is an independent noise source, the changes are not uniform. If the dominant noise source were column amps or row-

address circuitry, then the spatial noise would appear column- or row-correlated. The nature of 1/f noise in this regard is that it creates spatial noise that increases logarithmically with time. Because low-frequency noise generates effects that change slowly with time, use of a chopper effectively suppresses it.

Spatial noise is probably the limiting noise for all current DC-coupled uncooled IR sensors. Only AC-coupled ferroelectric devices have sufficiently low spatial noise to be limited by temporal noise. As the sensitivity of thermal detectors improves, the removal of spatial noise will become even more challenging.

SUMMARY AND CONCLUSIONS

Development of background-limited thermal detectors will be a substantial challenge. It will require clever design to include an efficient IR absorber in a very low-mass pixel structure. The detector device will have to be of sufficiently high impedance to avoid degradation of performance as the result of high-resistance in the electrical conduits. Success of background-limited devices will require development of low-cost vacuum technology capable of maintaining an ambient pressure of around 1 mTorr for the life of the product. Other issues, such as excessive self-heating in a bolometer of very low mass and very high thermal isolation, could prove detrimental to achieving the ultimate performance.

However, provided we are willing to modestly cool our thermal detectors, they potentially have essentially the same performance limits as photon detectors. Spectral band limiting by the IR absorber reduces the background noise limit in a manner not considered in past projections that showed thermal detectors to have a significant performance disadvantage. It is apparent that thermal detectors may even have an advantage for low-frequency applications, whereas photon detectors offer an advantage for high frequencies. Once thermal detectors are cooled, they are subject to the same benefits of cold shielding as are photon detectors. Note, however, that reducing the radiant emission of the detector and the background reduces both thermal conductance and noise. This will put further stress on detector mass, package vacuum and other noise components. This is not unexpected, of course, because reducing the limiting noise always makes other noise components more important.

To take advantage of the improvements, these future detectors must effectively suppress spatial noise. This means that such ultra-high-performance sensors will likely use AC-coupled detectors such as thin-film ferroelectric devices.

Many challenges lie ahead for continued progress in uncooled thermal detectors, but so also do many opportunities to dramatically improve the performance and utility of these devices. With sustained investment, thermal detectors will be able to serve the most stringent IR imaging applications currently served by low-temperature photon detectors, but thermal detectors will do it with substantially reduced cost, weight, and power.

---

[1] C.M. Hanson, "Analysis of the Effects of 1/f Noise and Choppers on the Performance of DC-Coupled Thermal Imaging Systems", **Infrared Technology and Applications XXVII, SPIE Vol. 4369**, p. 360.